Cellular/Molecular

Plasticity of Intrinsic Excitability during Long-Term Depression Is Mediated through mGluR-Dependent Changes in I_h in Hippocampal CA1 Pyramidal Neurons

Darrin H. Brager and Daniel Johnston
Center for Learning and Memory, University of Texas at Austin, Austin, Texas 78712

Bidirectional changes in synaptic strength are the proposed cellular correlate for information storage in the brain. Plasticity of intrinsic excitability, however, may also be critical for regulating the firing of neurons during mnemonic tasks. We demonstrated previously that the induction long-term potentiation was accompanied by a persistent decrease in CA1 pyramidal neuron excitability (Fan et al., 2005). We show here that induction of long-term depression (LTD) by 3 Hz pairing of back-propagating action potentials with Schaffer collateral EPSPs was accompanied by an overall increase in CA1 neuronal excitability. This increase was observed as an increase in the number of action potentials elicited by somatic current injection and was caused by an increase in neuronal input resistance. After LTD, voltage sag during hyperpolarizing current injections and subthreshold resonance frequency were decreased. All changes were blocked by ZD7288 (4-ethylphenylamino-1,2-dimethyl-6-methylaminopyrimidinium chloride), suggesting that a physiological loss of dendritic h-channels was responsible for the increase in excitability. Furthermore, block of group 1 metabotropic glutamate receptors (mGluRs) or protein kinase C prevented the increase in excitability, whereas the group 1 mGluR agonist DHPG [(*RS*)-3,5-dihydroxyphenylglycine] mimicked the effects. We conclude that 3 Hz synaptic stimulation downregulates I_h via activation of group 1 mGluRs and subsequent stimulation of protein kinase C. We propose these changes as part of a homeostatic and bidirectional control mechanism for intrinsic excitability during learning.

Key words: **H-channels; LTD; metabotropic; rat; PKC; DHPG**

Introduction

Information processing in the brain requires neurons and neuronal networks to continuously undergo changes in their input–output properties. Synaptic efficacy is a well studied mechanism for regulating neuronal output, and increases and decreases in synaptic strength are believed to be the cellular substrates for learning and memory (Bliss and Collingridge, 1993; Bear, 1996). The ability to regulate excitability within a modifiable range is vital for maintaining the computational power of the neuron. Although many studies have focused on morphological, biochemical and physiological changes that occur within or near synapses, recent studies examined changes in voltage-gated channels (Wang et al., 2003; Frick et al., 2004; Fan et al., 2005; Xu et al., 2005; Kim et al., 2007). The resulting influence on the active and passive membrane properties is called plasticity of intrinsic excitability (Frick and Johnston, 2005). The regulation of voltage-dependent ion channels by activity may represent a homeostatic mechanism for maintaining neuronal excitability within physiological limits (Abbott and Nelson, 2000; Turrigiano and Nelson, 2000). Because of its role in the regulation of membrane excitability, the hyperpolarization activated, nonselective cation channel (I_h) is a suitable candidate.

H-channels, first characterized in cardiac tissue, are widely distributed in the CNS (DiFransesco, 1993; Pape, 1996). I_h is a mixed-cation conductance with slow kinetics (CA1 pyramidal neurons, $\tau_{act} = 20$ ms; $\tau_{deact} = 18$ ms) (Magee, 1998). I_h contributes to synchronized network oscillations, intrinsic oscillations, and pacemaker activity in the thalamus, hippocampus, and neocortex (Hutcheon et al., 1996; Maccaferri and McBain, 1996; Lüthi et al., 1998). Because a significant amount is active a rest, I_h contributes to the resting membrane potential (Magee, 1998; Aponte et al., 2006). Furthermore, with its unique activation by hyperpolarization, I_h opposes changes in membrane potential and strongly influences synaptic integration (Magee, 1998; Magee, 1999). Although the h-channel has a relatively small single channel conductance compared with many other channels (Magee and Johnston, 1995; Chen and Johnston, 2004; Kole et al., 2006), the high density of h-channels in the dendrites, which increases with distance from the soma (Magee, 1998), contributes significantly to the total membrane conductance of the neuron. Subtle modifications in the physiology of h-channels can therefore produce significant changes in intrinsic excitability.

We used a long-term depression (LTD) protocol that con-

Received Aug. 2, 2007; revised Sept. 25, 2007; accepted Sept. 27, 2007.

This work was supported by National Institutes of Health Grants MH48432, MH44754, and NS37444 (D.J.). We thank R. Narayanan for technical assistance with the analyses of resonance frequency and the neuron simulations, R. A. Chitwood and J. A. Rosenkranz for helpful discussions, and members of the Center for Learning and Memory for critical review of this manuscript.

Correspondence should be addressed to Dr. Darrin H. Brager, Center for Learning and Memory, University of Texas at Austin, 1 University Station, C7000, Austin, TX 78712-0805. E-mail: dbrager@mail.clm.utexas.edu.

DOI:10.1523/JNEUROSCI.3520-07.2007

 0270-6474/07/2713926-12$15.00/0

sisted of pairing back-propagating action potentials and Schaffer collateral EPSPs at 3 Hz (Christie et al., 1996). In addition to producing LTD of EPSPs, 3 Hz pairing also resulted in a long-lasting increase in CA1 pyramidal neuron excitability. This increase was caused by a downregulation of I_h, because it was accompanied by changes in multiple electrophysiological measurements sensitive to I_h and was blocked by the I_h blocker ZD7288 (4-ethylphenylamino-1,2-dimethyl-6-methylaminopyrimidinium chloride). Furthermore, the decrease in I_h was blocked by group 1 mGluR antagonists and inhibitors of protein kinase C and was mimicked by application of a group 1 mGluR agonist. We suggest that activity-dependent increases in intrinsic excitability mediated by decreases in I_h act in a homeostatic manner to prevent the loss of neuronal output during hippocampal long-term depression.

Materials and Methods

Acute hippocampal slices. All experiments were conducted in accordance with the University of Texas at Austin Institutional Animal Care and Use Committee. Hippocampal slices (350 μm) were prepared from 4- to 6-week-old male Sprague-Dawley rats using standard techniques (Magee and Johnston, 1997). Briefly, animals were anesthetized using a lethal dose of ketamine and xylazine. Once deeply anesthetized, animals were perfused intracardially with ice-cold modified ACSF containing (in mM) 210 sucrose, 2.5 KCl, 1.2 NaH_2PO_4, 25 $NaHCO_3$, 0.5 $CaCl_2$, 7.0 $MgCl_2$, and 7.0 dextrose bubbled with 95%O_2/5%CO_2. The brain was removed and bisected along the midline. To promote an orientation favoring dendritic projection in a plane parallel to the surface of the slice, an additional cut was made on the dorsal surface at a 30° angle lateral to the midline. The brain was mounted and sliced using a microtome (Vibratome, St. Louis, MO). Slices were placed in a holding chamber filled with ACSF containing (mM) 125 NaCl, 2.5 KCl, 1.25 NaH_2PO_4, 25 $NaHCO_3$, 2 $CaCl_2$, 2 $MgCl_2$, and 25 dextrose (see below) warmed to 35°C for 20 min and then placed at room temperature for <6 h until needed for recording.

Electrophysiology. For all recordings, the control ACSF solution contained (mM) 125 NaCl, 2.5 KCl, 1.25 NaH_2PO_4, 25 $NaHCO_3$, 2 $CaCl_2$, 1 $MgCl_2$, and 25 dextrose and was bubbled continuously with 95%O_2/5%CO_2 at 31–33°C. Slices were placed individually as needed into a submerged recording chamber continuously perfused with control extracellular saline. Slices were viewed with a Zeiss (Oberkochen, Germany) Axioskop using infrared video microscopy and differential interference contrast (DIC) optics. In those experiments examining LTD of EPSPs, $GABA_A$-mediated inhibition was blocked by inclusion of 10 μM bicuculline and 10 μM picrotoxin in the extracellular saline. In these cases, area CA3 was removed before placing the slice in the recording chamber to prevent spontaneous epileptiform-like discharge. Patch pipettes were pulled from borosilicate glass and had a resistance of 4–8 MΩ when filled with the internal recording solution containing (in mM) 120 potassium methanesulfonate or potassium methylsulfate, 20 KCl, 10 HEPES, 4 NaCl, 0.2 EGTA, 4 MgATP, 0.3 TrisGTP, and 14 phosphocreatine, pH 7.3 (with KOH).

All whole-cell recordings were made from the soma or along the first 50 μm of the proximal apical dendrite of CA1 pyramidal neurons using a Dagan (Minneapolis, MN) BVC-700 in current-clamp mode. Series resistance was monitored throughout the recording and experiments in which the series resistance exceeded 30 MΩ were discarded. EPSPs of 4–6 mV were elicited using tungsten bipolar stimulating electrodes (180–220 μA for 0.1 ms) placed near (<20 μm) the main apical dendrite ~150–180 μm from the soma in stratum radiatum. Back-propagating action potentials (b-APs) were elicited by current injection into the soma (1–2 nA for 2 ms) or by antidromic extracellular stimulation. LTD was induced by pairing EPSPs and b-APs at 3 Hz for 5 min (Christie et al., 1996).

Data acquisition and analysis. Data were sampled at 10 kHz, filtered at 3 kHz and digitized by an ITC-18 interface connected to computer running custom software written in IgorPro (Wavemetrics, Lake Oswego, OR). All data analyses were performed with custom written software in IgorPro (Wavemetrics). EPSPs were quantified by measuring the initial slope (linear fit over 1–2 ms). The EPSP slope provides a better measure of synaptic transmission than EPSP amplitude because of the potential contribution of voltage-dependent conductances to the amplitude of the EPSP. Input resistance (R_N) was determined by the slope of the linear regression line through the *V–I* plot (fit through the linear range of a plot of the amplitude of the steady-state voltage against the corresponding current injection from a family of 500–750 ms current steps). Input–output curves were constructed by plotting the numbers of action potentials against the amplitude of the current injections (150–300 pA, for 500 ms in 50 pA intervals). Action potential threshold was defined as the voltage where the first derivative of the voltage (dV/dt) first exceeds 10 mV/ms (Fan et al., 2005). Estimates of the membrane time constant (τ_m) were made by fitting a single exponentials to the same family of voltage responses used for input resistance measurements and calculating the average τ_m. Exponentials were fit to relaxation of the membrane voltage over a 25 ms window beginning 2 ms after the end of the current injection.

For measurements of temporal summation, simulated EPSPs (αEPSPs) were used to remove any contribution of presynaptic mechanisms. αEPSPs were simulated by the injection of current using the following function: $I = I_{max}(t/\alpha)e^{-\alpha t}$. I_{max} and α were adjusted to produce EPSP-like waveforms with a peak amplitude of 5 mV and a time-to-peak of 10 ms similar to evoked EPSPs. Temporal summation ratio was measured as the amplitude of the fifth αEPSP relative to first in a train of 5 αEPSPs [($\alpha EPSP_5 - \alpha EPSP_1$)/$\alpha EPSP_1$].

Voltage sag was measured as the percentage change between the maximum and steady state voltage change during hyperpolarizing current injections [($V_{max} - V_{ss}$)/V_{max}] × 100. The stimulus used for characterizing the impedance amplitude profile (ZAP) was a sinusoidal current of constant amplitude (50 or 100 pA), with its frequency linearly spanning 0–15 Hz in 15 s. The magnitude of the ratio of the Fourier transform of the voltage response to the Fourier transform of the current stimulus formed the impedance amplitude profile. The frequency at which the impedance amplitude reached its maximum was the resonance frequency.

Statistical analyses. All data are expressed as mean ± SEM. Statistical comparisons were made using ANOVA (one-way, two-way or repeated measures design as appropriate) followed by Tukey–Kramer multiple-comparisons *post hoc* test or Student's *t* test (paired or unpaired as appropriate) with InStat software. Linear fits and correlations were made using either Igor (Wavemetrics) or InStat (GraphPad, San Diego, CA). Data were considered statistically significant if $p < 0.05$.

Drugs and solutions. All drugs were made from stock solutions in water, equivalent NaOH, or DMSO (final concentration of DMSO ≤0.1%) accordingly. ZD7288, D, L-APV, (+)-MK-801 maleate, CNQX, bicuculline, picrotoxin, (2*S*)-2-amino-2-[(1*S*,2*S*)-2-carboxycycloprop-1-yl]-3-(xanth-9-yl) propanoic acid (LY341495), (*RS*)-3,5-dihydroxyphenylglycine (DHPG), and GF109203X were obtained from Tocris Cookson (Bristol, UK). When 20 mM K_4-BAPTA (Sigma, St. Louis, MO) was including in the recording pipette, potassium methylsulfate or methanesulfonate was reduced to 40 mM and the osmolality adjusted with sucrose.

Results

LTD is accompanied by increased CA1 pyramidal neuron excitability

Long-term depression of CA3-CA1 synaptic transmission was induced by delivering a train of b-APs paired with synaptic stimulation at 3 Hz for 5 min (900 total b-AP–EPSP pairs; b-AP preceded EPSP by 5 ms) (Christie et al., 1996). All measurements were made at 31–33°C and the holding current was adjusted to keep the membrane potential at −70 mV. The membrane potential was allowed to vary during the pairing protocol. Three hertz pairing resulted in a significant decrease in EPSP slope that persisted for the duration of recordings (Fig. 1*A*). In the absence of the induction protocol, there was no significant change in EPSP slope. The 3 Hz pairing was accompanied by increased CA1 pyramidal neuron excitability measured as the number action po-

tentials elicited by a given current injection (Fig. 1*B*,*C*). The number of action potentials elicited by current injection in the soma increased at all injection amplitudes after LTD induction (Fig. 1*C*). The underlying cause for this increase in APs per current injection was an increase in CA1 pyramidal neuron input resistance. Input resistance (R_N) increased by 87 ± 10% after 3 Hz pairing (baseline, 54 ± 3 MΩ; 3 Hz, 99 ± 5MΩ; $n = 20$; $p < 0.001$) (Fig. 1*D*). We also found that the membrane time constant (τ_m) was significantly increased after 3 Hz pairing (baseline, 21 ± 2 ms; 3 Hz pairing, 28 ± 2 ms; $p < 0.005$) (supplemental Fig. 1, available at www.jneurosci.org as supplemental material). There was a small but significant increase in input resistance (R_N) in the absence of the pairing protocol (Fig. 1*D–F*). A previous report on the effects of internal anions on intrinsic membrane properties suggests that methylsulfate based internal recording solutions can increase R_N during whole-cell recording (Kaczorowski et al., 2007). Although we observed this as well, the effect of dialysis was significantly smaller than the increase in R_N after 3 Hz pairing (Fig. 1*D–F*). The increase in AP firing was not likely caused by alterations in sodium channel activation as there was no significant change in action potential threshold after 3 Hz pairing (baseline, −50.7 ± 0.6 mV; 3 Hz, −52.9 ± 1.5 mV; $n = 5$, $p = 0.2$). CA1 pyramidal neuron input resistance increased gradually after LTD induction reaching an apparent plateau ~30 min after 3 Hz pairing (Fig. 1*E*). A plot of input resistance versus EPSP slope, measured for 30 min after 3 Hz pairing, revealed a linear correlation ($r = -0.85$; $n = 13$; $p < 0.001$) between the decrease in synaptic strength and the increase in input resistance (Fig. 1*F*). We described a similar correlation in CA1 pyramidal cells between the decrease in input resistance and magnitude of the increase in EPSP slope after LTP induction (Fan et al., 2005).

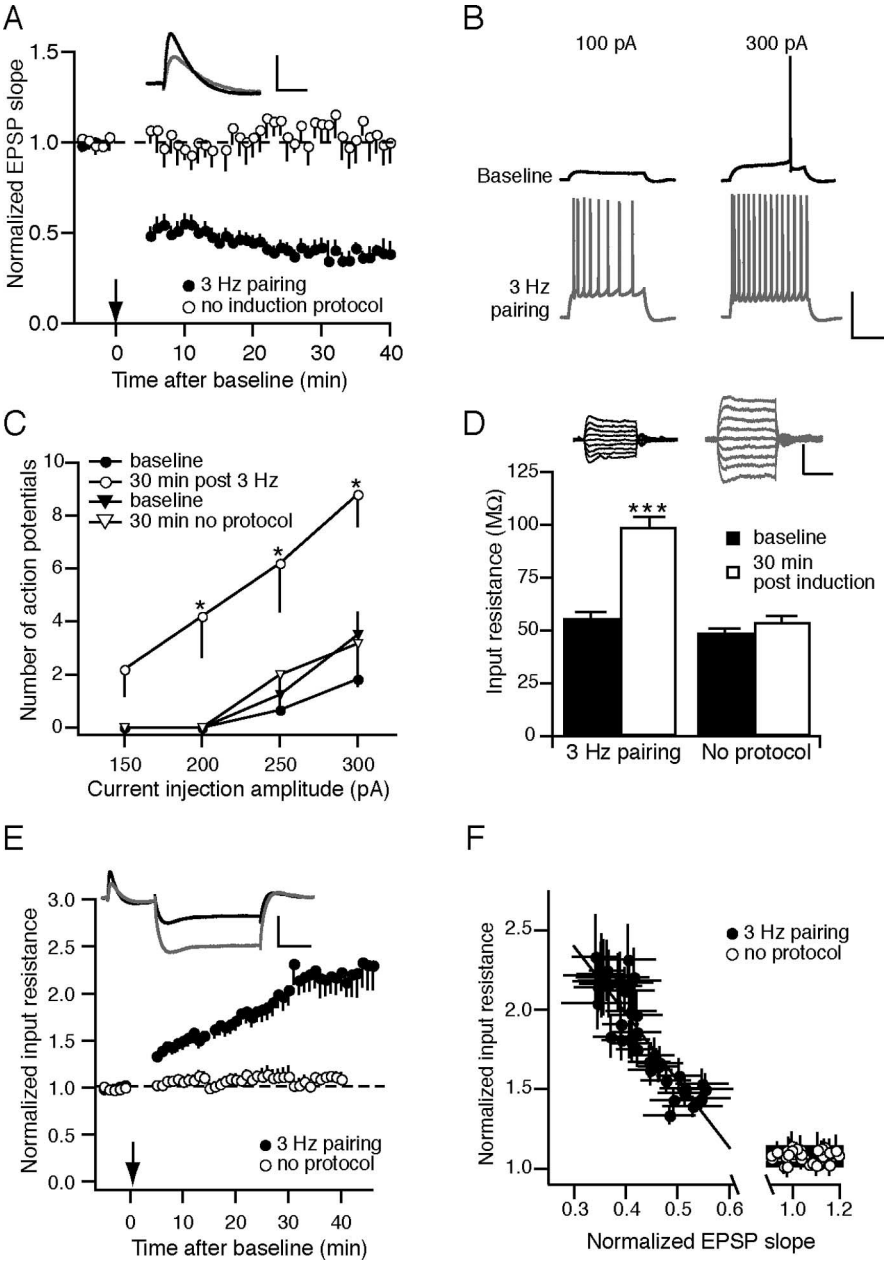

Figure 1. 3 Hz pairing of b-APs and EPSPs produces LTD and a persistent increase in neuronal excitability and input resistance. ***A***, Graph showing the time course and magnitude of the change in EPSP slope after either 3 Hz pairing (●; $n = 20$) or whole-cell control (○; $n = 7$). Note that 3 Hz pairing consisted of a 5 min train of 900, b-AP–EPSP pairs (↓). The inset shows representative EPSPs during the baseline period (black) and 30 min after 3 Hz pairing (gray). Calibration: 3 mV, 50 ms. ***B***, Representative voltage recordings during a 500 ms injection of either 100 or 300 pA before (black) and 30 min after (gray) 3 Hz pairing. Calibration: 50 mV, 200 ms. ***C***, Summary data showing action potential firing elicited by somatic current injection before (●) and 30 min after (○) 3 Hz pairing ($n = 5$). There was no significant change in AP firing in the absence of 3 Hz pairing (baseline, ▼; 30 min, ▽). ***D***, Summary data showing increased R_N 30 min after 3 Hz pairing ($n = 20$) but not during whole-cell control recordings ($n = 10$). Inset, Representative voltage deflections in response to a series of current steps (−40 to +40 pA) before (black) and 30 min after 3 Hz pairing (gray). Calibration: 3 mV, 250 ms. ***E***, Graph showing the time course and magnitude of the change in input resistance after either 3 Hz pairing (●; $n = 13$) or whole-cell control (○; $n = 7$). Inset, Representative traces before (black) and after (gray) 3 Hz pairing showing both EPSP depression and increased input resistance after 3 Hz pairing. Note that for these measurements, input resistance was measured by a single −50 pA injection. Calibration: 5 mV, 150 ms. ***F***, Relationship between R_N and EPSP slope after either 3 Hz pairing (●; $n = 13$) or in the absence of the 3 Hz protocol (○; $n = 7$). There was a strong linear correlation ($r = -0.86$) between R_N slope and EPSP slope after 3 Hz pairing. Error bars indicate SEM. *$p < 0.05$; ***$p < 0.005$ baseline versus 30 min after 3 Hz pairing.

Downregulation of I_h underlies increased CA1 pyramidal neuron excitability

An increase in I_h is responsible for the decrease in input resistance that accompanies LTP (Fan et al., 2005). Accordingly, we hypothesized that a decrease in I_h would explain our observation of increased input resistance after 3 Hz pairing. Furthermore, 3 Hz pairing resulted in a hyperpolarization of the resting membrane potential (baseline, −69 ± 2 mV; 3 Hz, −74 ± 2 mV; $n = 10$; $p < 0.01$), consistent with a decrease in I_h (Gasparini and DiFrancesco, 1997). To explore the role of I_h in the increased excitability associated with LTD, the 3 Hz pairing paradigm was repeated in the presence of the I_h blocker ZD7288 (20 μM). Because there is a significant amount of I_h active at rest in CA1 pyramidal cells, I_h contributes to the resting input resistance

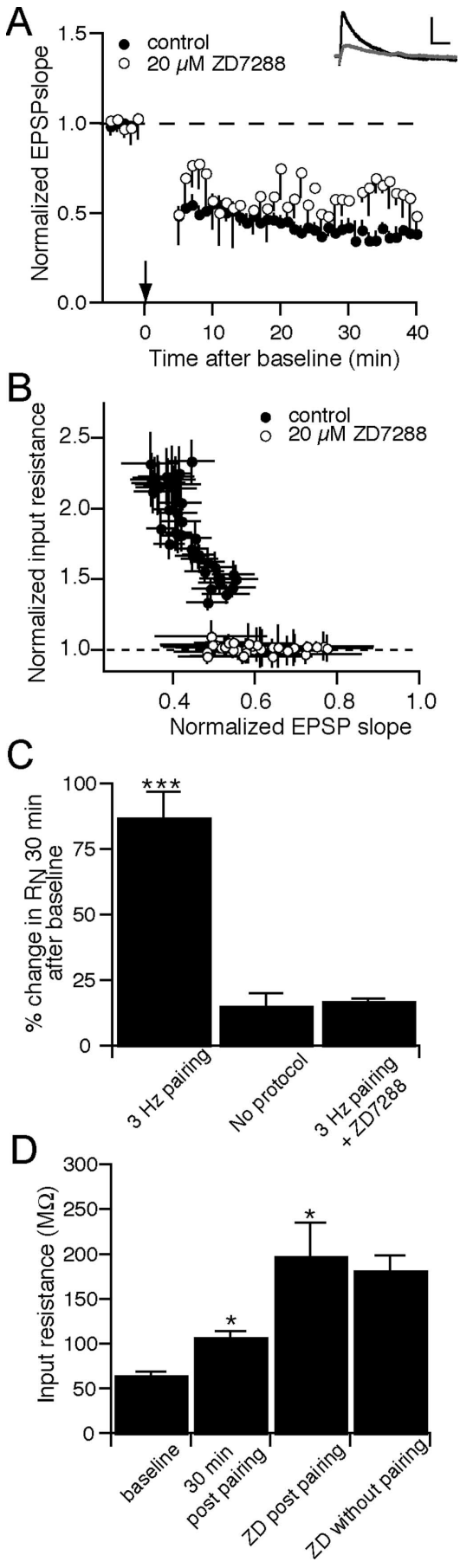

(Magee, 1998). As expected, block of I_h with ZD7288 resulted in a 180% increase in CA1 pyramidal neuron input resistance (initial, 77 ± 15 MΩ; 30 min, 211 ± 35 MΩ; $n = 4$; $p < 0.05$). Although we observed no significant effect on EPSP slope by ZD7288 (data not shown) (cf. Chevaleyre and Castillo, 2002), we nonetheless sought to remove any presynaptic influences by including ZD7288 in the postsynaptic recording electrode. Block of I_h by postsynaptic application of ZD7288 did not significantly affect the decrease in EPSP slope after 3 Hz pairing (LTD in control, 40 ± 4%; LTD in ZD7288, 55 ± 10%; $p > 0.05$) (Fig. 2*A*). However, there was no further increase in R_N after 3 Hz pairing (Fig. 2*B*,*C*). If 3 Hz pairing increases R_N by downregulating I_h, then the total increase in R_N induced by 3 Hz pairing followed by ZD7288 application should be the same as the total increase in R_N when ZD7288 is applied to naive CA1 pyramidal cells. In a separate set of experiments, ZD7288 was applied extracellularly 30 min after the 3 Hz pairing induced increase in input resistance (Fig. 2*D*). After 3 Hz pairing, R_N significantly increased by 43 ± 8MΩ ($p < 0.05$, $n = 4$). Application of ZD7288 further increased R_N, for a total increase of 133 ± 36 MΩ. Application of ZD7288 to naive slices increased R_N by 126 ± 26 MΩ ($n = 4$) and was not significantly different from the ZD induced increase after 3 Hz pairing (Fig. 2*D*). These results suggest that 3 Hz pairing results in the physiological loss of a significant fraction of CA1 pyramidal neuron I_h.

A loss of I_h should result in longer EPSP decay times and increases in temporal summation (Magee, 1999). We previously showed activity-dependent increases in I_h after LTP were accompanied by decreases in EPSP decay time and temporal summation (Fan et al., 2005). After 3 Hz pairing, EPSP decay time increased significantly. The increase in decay time was blocked by ZD7288 and absent when there was no induction protocol (Fig. 3*A*). One potential problem of these experiments is that a decrease in EPSP amplitude alone should increase decay time as smaller EPSPs will deactivate I_h less than larger EPSPs. Simply increasing the stimulation intensity to return EPSP amplitude to control levels, however, could present additional problems, because this could recruit new synapses that did not undergo plasticity. To address this issue, we stimulated two nonoverlapping pathways that made synapses onto the same CA1 pyramidal neuron to compare the change in EPSP slope and decay after 3 Hz pairing. 3 Hz pairing induced a significant decrease EPSP slope in the test pathway compared with the control pathway (34 ± 2% vs 97 ± 3%) (Fig. 3*B*,*C*). As expected, there was a significant increase in input resistance after 3 Hz pairing (43 ± 11 MΩ; 3 Hz, 84 ± 19 MΩ; $p < 0.05$). Accordingly, there was a linear correlation between the increase in input resistance and the decrease in EPSP slope of the test pathway but not the control pathway (Fig. 3*D*). Interestingly, the 10–90% decay time of the both the test and control EPSPs was

Figure 2. Blockade of h-channels occluded the increase in excitability but had no effect on synaptic depression. ***A***, Graph showing the time course and magnitude of EPSP depression from control slices (●; $n = 20$) and when 20 μM ZD7288 was included in the recording pipette (○; $n = 5$). Inset, Representative traces from the baseline (black) and 30 min after 3 Hz pairing (gray) showing that pairing still produced depression of EPSPs with intracellular ZD7288 (20 μM). Calibration: 2 mV, 25 ms. ***B***, The relationship between R_N and EPSP slope after 3 Hz pairing from control experiments (●) and with ZD7288 in the recording pipette (○). Note that there was still depression of EPSP slope with ZD7288, but no increase in R_N. ***C***, Summary graph showing that 3 Hz pairing did not further increase R_N when h-channels were blocked with ZD7288. ***D***, Summary graph showing R_N measured during baseline, 30 min after 3 Hz pairing, and 30 min after extracellular application of ZD7288 (60 min after 3 Hz pairing; $n = 4$). For comparison, the R_N from a separate group of cells treated with extracellular ZD7288 only (no pairing) is shown ($n = 4$ cells). Error bars indicate SEM. *$p < 0.05$; ***$p < 0.005$.

significantly greater after 3 Hz pairing (Fig. 3*E*). Because the decay time was longer for control EPSPs despite no change in amplitude, we conclude that the increase in decay of depressed EPSPs is caused by the activity-dependent decrease in I_h as well as the decrease in EPSP amplitude.

To assess temporal summation, a train of five current pulses (modeled by an α function, αEPSPs) was used to mimic EPSPs. The use of αEPSPs removes any potential presynaptic components that may occur during repetitive stimulation (Brager et al., 2002). Five αEPSPs were injected into the soma at 5, 10, 20, and 50 Hz and summation was expressed as the percentage increase in the fifth EPSP relative to the first. Temporal summation was significantly increased during the 10 and 20 Hz trains, but not the 5 or 50 Hz trains after 3 Hz pairing (Fig. 3*F*). These intermediate frequencies are most sensitive to changes in I_h (Poolos et al., 2002).

These results suggest that the increase in input resistance after 3 Hz pairing was caused by a decrease in I_h. As an additional test of this hypothesis, two additional electrophysiological parameters sensitive to changes in I_h were examined: membrane potential sag (voltage sag) and resonance frequency (f_R). With its activation by hyperpolarization and deactivation by depolarization, I_h opposes changes in membrane potential. This is observed as the characteristic voltage sag after a depolarizing or hyperpolarizing change from rest (Poolos et al., 2002). This same characteristic allows I_h to act as a resonator conductance and changes in resonance frequency can reflect changes in I_h (Hutcheon and Yarom, 2000) (Narayanan and Johnston, 2007). Pharmacological block of I_h with ZD7288 resulted in increased input resistance, complete loss of voltage sag and a decrease in the resonance frequency (baseline, 3.8 ± 0.24 Hz; ZD7288, 1.2 ± 0.12 Hz; $p < 0.05$). If the observed increase in input resistance is caused by the physiological loss of I_h, a decrease in sag and resonance frequency after 3 Hz pairing would be expected.

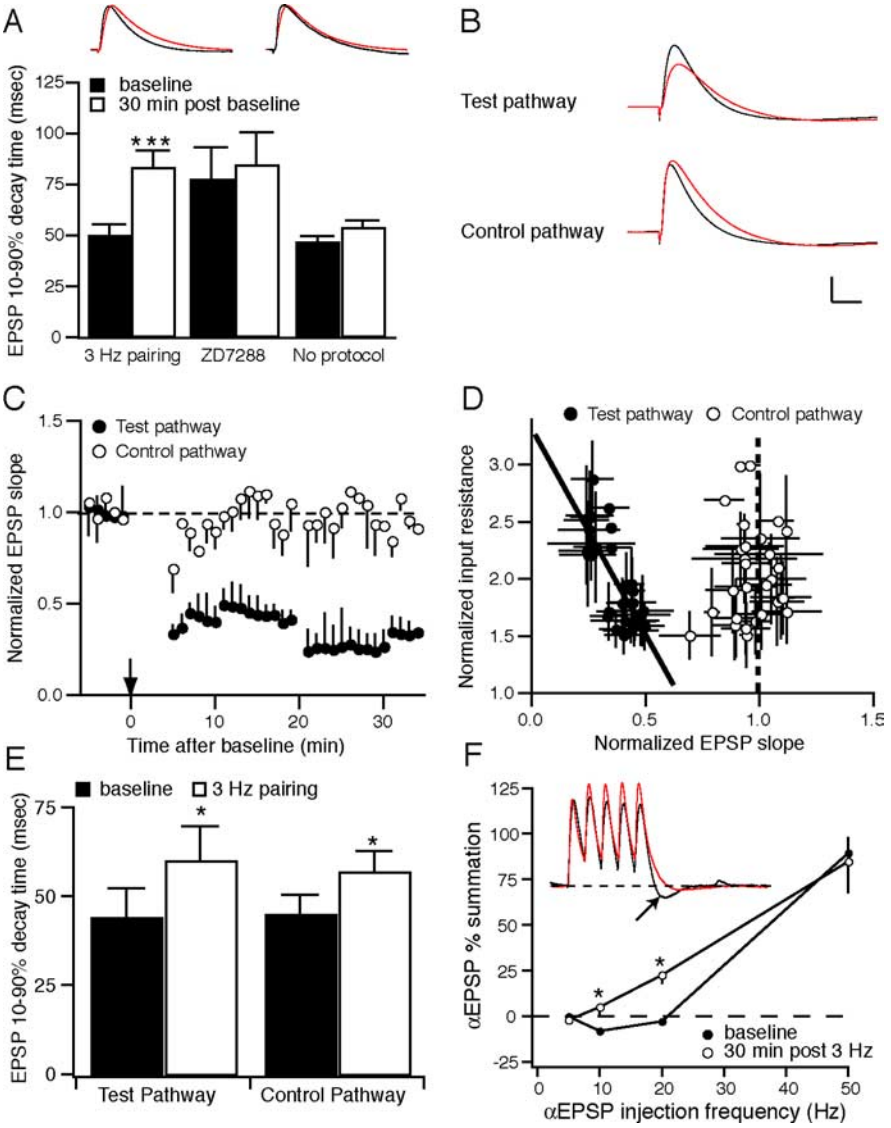

Figure 3. Increases in temporal summation accompany 3 Hz pairing induced LTD. ***A***, Summary graph showing that the 10–90% decay time of EPSPs was increased after 3 Hz pairing in control experiments ($n = 20$), but not with ZD7288 in the recording pipette ($n = 5$) or in whole-cell control experiments ($n = 7$). Inset, Representative traces from 3 Hz pairing (left) and whole-cell control experiments (right). Black traces are from the baseline period and red traces are from 30 min later. Note 30 min traces are scaled to the peak of the baseline traces to highlight changes in EPSP decay. ***B***, Representative traces showing EPSPs before (black) and after (red) 3 Hz pairing elicited from the test and control pathways onto the same cell. Note the increased decay in both the test and control EPSPs after 3 Hz pairing. Calibration: 2 mV, 25 ms. ***C***, Group data showing LTD of the test (●), but not the control (○) pathway ($n = 4$). The (↓) indicates the time of 3 Hz pairing. ***D***, Relationship between the increase in input resistance and EPSP slope for both the test (●) and control (○) pathways. ***E***, Summary data showing that EPSP 10–90% decay is significantly increased after 3 Hz pairing for both the test and control pathways. ***F***, Summary graph showing summation of αEPSPs before (●) and after (○) 3 Hz pairing ($n = 4$). There was a significant increase in summation at 10 and 20 Hz. Note a reduction in the undershoot (↓) after 3 Hz pairing indicative of a decrease in I_h. Inset, Representative traces showing αEPSP summation at 20 Hz before (black) and after (red) 3 Hz pairing. Traces are scaled to the first αEPSP to illustrate change in summation. Error bars indicate SEM. *$p < 0.05$; ***$p < 0.005$ baseline versus 30 min after 3 Hz pairing.

Voltage sag was measured from a family of hyperpolarizing current injections from the resting membrane potential measured before and after 3 Hz pairing. Because I_h is voltage-sensitive, sag was compared between two different current steps that had a similar peak voltage deflection (Fig. 4*A*). After 3 Hz pairing, voltage sag significantly decreased from 24 ± 2% to 9 ± 1% (Fig. 4*B*). Resonance frequency (f_R) was determined by recording the voltage response during injection of the ZAP current stimulus (Fig. 4*C*). The maximum of the impedance amplitude profile (see Materials and Methods) occurs at the resonant frequency of the cell (Fig. 4*D*). The f_R of CA1 pyramidal neurons was significantly decreased from 3.8 ± 0.4 Hz to 2.4 ± 0.5 Hz ($n = 9$; $p < 0.05$) after 3 Hz pairing (Fig. 4*E*). Neither voltage sag nor f_R changed significantly in the absence of 3 Hz pairing (Fig. 4*B*,*E*). As for the change in input resistance, the decrease in sag and resonance frequency after 3 Hz pairing was less than that observed after application of ZD7288. In combination, these results suggest that 3 Hz pairing results in a physiological loss of a fraction of the total I_h.

Although these data support the hypothesis that a decrease in I_h underlies the increase in input resistance, we cannot at this point rule out the loss of a voltage-independent conductance. If

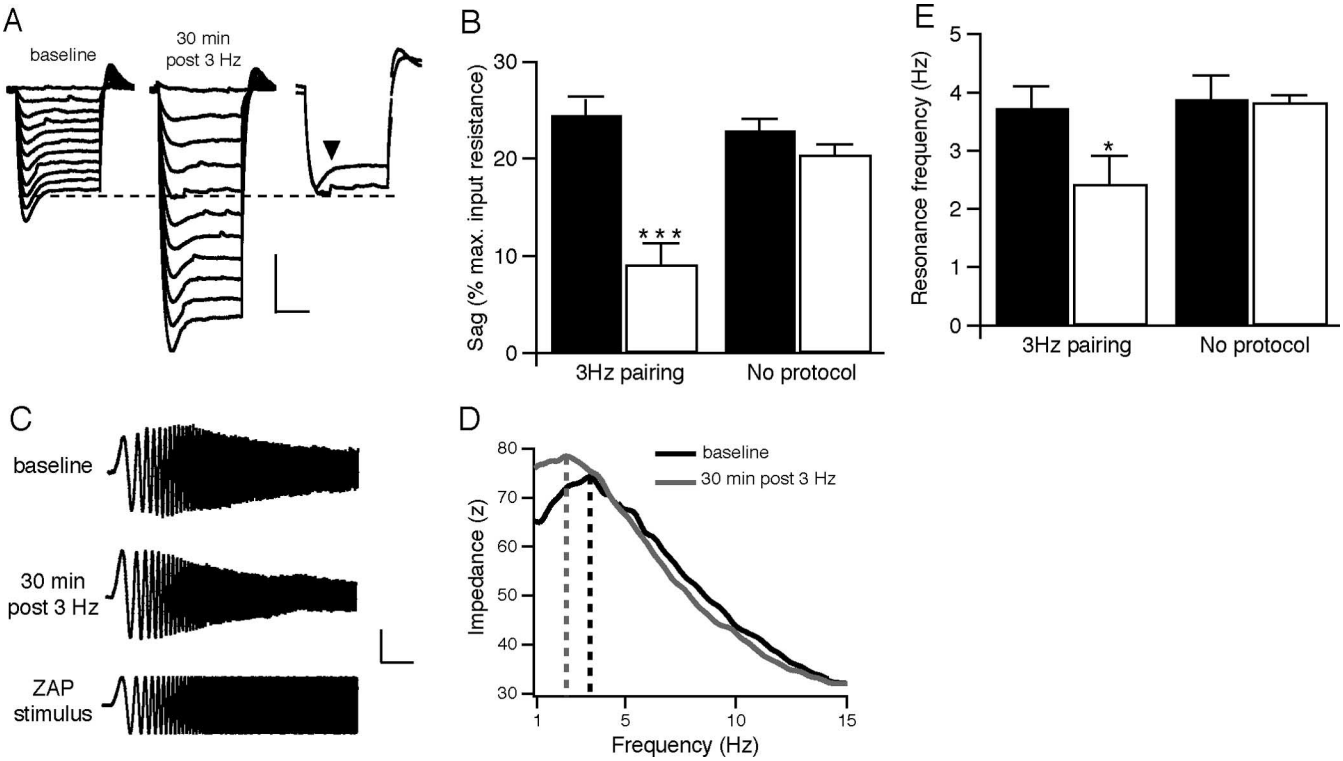

Figure 4. Electrophysiological measurements sensitive to I_h are altered after 3 Hz pairing. ***A***, Representative voltage traces in response to a series of hyperpolarizing current injections (0 to −200 pA) during the baseline period and 30 min after 3 Hz pairing. The traces on the right show current injections that produced the same maximum voltage deflection before and after 3 Hz pairing. Note that the prominent sag present before is significantly reduced after (▼). Calibration: 5 mV, 200 ms. ***B***, Summary graph showing decreased sag 30 min after 3 Hz pairing ($n = 10$), but not in whole-cell control experiments ($n = 10$). ***C***, Representative voltage traces during injection of the ZAP stimulus before and 30 min after 3 Hz pairing. The bottom trace shows the ZAP current stimulus. ***D***, Impedance amplitude profile showing a leftward shift of the maximum impedance after 3 Hz pairing. ***E***, Summary graph showing that resonance frequency is decreased after 3 Hz pairing ($n = 9$), but not whole-cell controls ($n = 3$). Error bars indicate SEM. *$p < 0.05$; ***$p < 0.005$ baseline versus 30 min after 3 Hz pairing.

the increase in input resistance was caused by a change in a voltage independent conductance (i.e., I_{leak}), then there should be no voltage dependence to the increase in R_N after 3 Hz pairing. CA1 pyramidal neuron input resistance was measured at various membrane potentials between −60 and −90 mV before and after 3 Hz pairing (Fig. 5*A*). The increase in input resistance was greater at the hyperpolarized membrane potentials. A fit of the normalized increase in R_N as a function of membrane potential had a slope of −0.22 and was significantly different from a slope of zero ($p < 0.005$; $n = 5$) (Fig. 5*B*). These results support the hypothesis that a change in a voltage-dependent conductance underlies the increase in input resistance after 3 Hz pairing. Although voltage sag during a hyperpolarizing injection can be used to estimate I_h, the rebound potential after the offset of the current can also be used. Other channels such as the inwardly rectifying potassium channel (I_{KIR}) will contribute to the steady-state voltage response during hyperpolarizing current injections. Because the deactivation of I_{KIR}, caused by the voltage-dependent block by Mg^{2+} ions, is fast (8–9 ms at 15°C) (Matsuda et al., 1987) compared with the deactivation of I_h, the rebound potential amplitude should be indicative of the amount of I_h activated at a given membrane potential. Given that long (500 ms) current injections were used to measure R_N and sag, the steady-state voltage can be treated as the new holding potential. We therefore plotted the rebound potential amplitude as a function of the steady-state voltage (Fig. 5*C*). The slope of the line fit to the data were decreased after 3 Hz pairing (baseline, −0.31 ± 0.007; 3 Hz, −0.15 ± 0.006; $n = 16$) (Fig. 5*D*). In the absence of 3 Hz pairing, there was no significant change in rebound potential amplitude as a function of membrane potential (baseline, −0.31 ± 0.005; 30 min, −0.27 ± 0.008; $n = 8$). These results suggest that after 3 Hz pairing, I_h is reduced because the h-conductance (g_h) is smaller.

The reduction in g_h after 3 Hz pairing could be caused by a hyperpolarizing shift in the activation of I_h (shift in $V_{1/2}$), a decrease in the maximum conductance (g_{max}) or a combination of both. A plot of resonance frequency (f_R) as a function of holding potential should produce a bell-shaped relationship that is well described by the first derivative of the Boltzmann function (supplemental Fig. 2, available at www.jneurosci.org as supplemental material). Shifts in the voltage dependence of this relationship can be used to make estimates of changes in g_{max} and $V_{1/2}$ of I_h (Narayanan and Johnston, 2007). A change in the voltage where the maximum resonance frequency occurs (V_B) reflects a shift in $V_{1/2}$; changes in maximum resonance frequency reflect a difference in g_{max} (supplemental Fig. 2, available at www.jneurosci.org as supplemental material). The f_R of CA1 pyramidal neurons ($n = 5$) was measured at six membrane potentials between −60 and −90 mV before and after 3 Hz pairing. As the membrane potential was hyperpolarized, f_R increased because of an increase in the proportion of active h-channels (Fig. 5*E*). Fitting the group data with the derivative of the Boltzmann revealed that the maximum resonance frequency was decreased from 6.6 to 5.3 Hz, consistent with a decrease in g_{max} (Fig. 5*F*). Although, the voltage where the maximum resonance frequency occurred was shifted toward hyperpolarized potentials (baseline, −80.4 ± 0.5 mV; 3 Hz pairing, −83.6 ± 2 mV; $n = 5$), this difference was within sampling error (f_R was measured in 5 mV intervals). These data support the hypothesis that a decrease in I_h occurs after 3 Hz

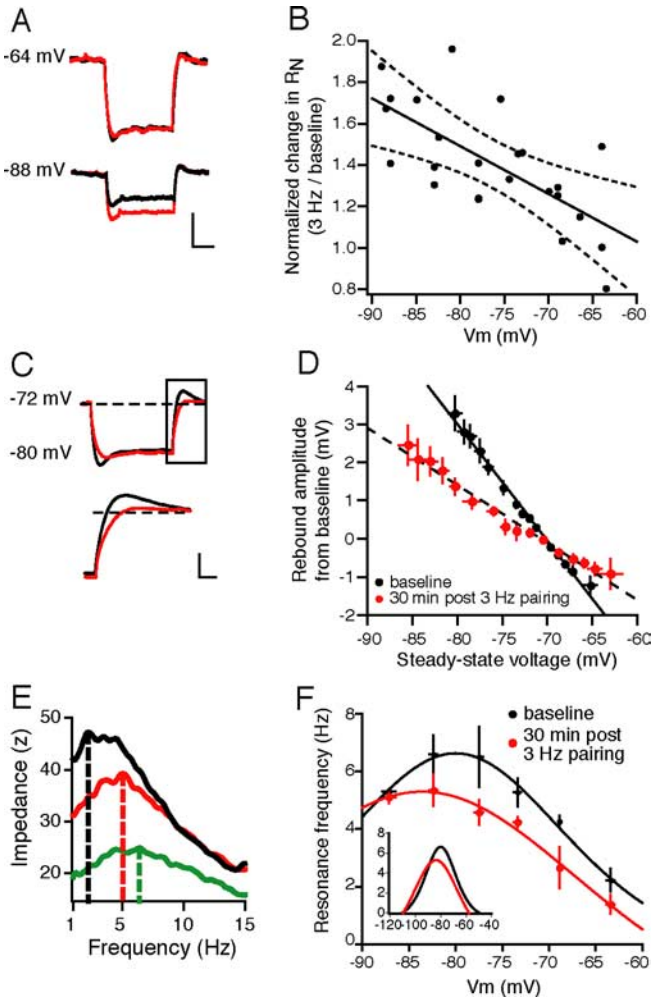

Figure 5. Voltage dependence of the changes in input resistance, rebound potential, and resonance frequency after 3 Hz pairing suggest a decrease in I_h. ***A***, Representative traces showing the measurement of R_N before (black) and after (red) 3 Hz pairing at the indicated membrane potentials. Note the lack of change at −64 mV compared with −82 mV. Calibration: 2 mV, 150 ms. ***B***, Summary graph showing the normalized change in input resistance as a function of membrane potential ($n = 5$). There was a strong negative correlation between the change in R_N and membrane potential (linear fit, solid line; confidence bands, dashed lines). ***C***, Representative traces showing the rebound potential amplitude before (black) and after (red) 3 Hz pairing. The bottom traces are expanded from the indicated region above. Calibration: top, 4 mV, 100 ms; bottom, 3 mV, 25 ms. ***D***, Summary graph showing rebound potential amplitude as a function of membrane potential before (●) and after (red filled circle) 3 Hz pairing. The intersection of the lines occurs near the holding potential of the neuron. ***E***, Representative graph showing the impedance amplitude profile measured at three membrane potentials (black, −63 mV; red, −71 mV; green, −82 mV). Note the rightward shift of the maximum impedance consistent with an increase in resonance frequency (dashed lines). ***F***, Summary graph showing measured resonance frequency as a function of membrane potential before (●) and after (red filled circle) 3 Hz pairing ($n = 5$). Solid lines fits of experimental data by the first derivative of the Boltzmann. Inset, Fits of the experimental data shown across the voltages used during the simulations in supplemental Figure 2 (available at www.jneurosci.org as supplemental material). Error bars indicate SEM.

pairing. Furthermore, these data suggest that a decrease in g_{max} underlies the reduction in I_h although we cannot rule out changes in $V_{1/2}$ (see Discussion). These results together with the sensitivity to ZD7288, the increase in input resistance, hyperpolarization of resting V_m, and increase in temporal summation and EPSP decay support the hypothesis that the increase in CA1 pyramidal neuron excitability after 3 Hz pairing is caused by the activity-dependent downregulation of I_h.

Increased excitability requires mGluR activation

Hippocampal LTD requires the activation of either NMDA receptors (NMDARs) (Dudek and Bear, 1992; Mulkey and Malenka, 1992; Bliss and Collingridge, 1993; Christie et al., 1996; Oliet et al., 1997; Malenka and Bear, 2004) and/or metabotropic glutamate receptors (mGluRs) (Bolshakov and Siegelbaum, 1994; Selig et al., 1995; Oliet et al., 1997; Huber et al., 2000; Normann et al., 2000; Rammes et al., 2003). We previously described a role for NMDA receptors in the plasticity of h-channels during LTP (Fan et al., 2005). H-channels have not been shown previously to undergo either NMDAR- or mGluR-dependent modulation during LTD.

Decreased CA1 pyramidal neuron excitability after LTP induction required Ca^{2+} influx via NMDA receptor activation (Fan et al., 2005). The increase in CA1 pyramidal neuron excitability that accompanied LTD is similarly Ca^{2+}-dependent because the inclusion of 20 mM BAPTA in the recording pipette blocked the increase in input resistance (Fig. 6*A*,*B*). The activation of both NMDA receptors and mGluRs can occur during LTD inducing protocols (Oliet et al., 1997; Huber et al., 2002). To determine whether the activation of these receptors is required for the activity-dependent downregulation of I_h, we repeated the 3 Hz pairing in the presence of either 50 μM D, L-APV and 10 μM (+)-MK-801, to block NMDA receptors, or 100 μM LY341495 to block mGluR receptors. These antagonists are known to block NMDA- and mGluR-dependent LTD respectively (Oliet et al., 1997; Huber et al., 2000, 2002). Bath application of either APV/MK-801 or LY341495 reduced LTD of EPSP slope (Fig. 6*C*). This suggests that the activation of both NMDA and mGluRs occurs during the 3Hz pairing-induction of LTD. APV/MK-801 had no effect on the increase in input resistance (Fig. 6*D–F*) or on the decrease in voltage sag (baseline, 23 ± 2%; 3 Hz, 15 ± 2%; $n = 8$, $p < 0.05$) after 3 Hz pairing. In contrast, LY341495 significantly reduced the increase in input resistance after 3 Hz pairing (Fig. 6*D–F*) and the decrease in voltage sag (baseline, 22 ± 2%; 3 Hz, 19 ± 2%; $n = 5$, $p > 0.05$). The increase in τ_m was also blocked by LY341495 but not APV/MK-801 (supplemental Fig. 1, available at www.jneurosci.org as supplemental material). These results suggest that activation of mGluRs during 3 Hz pairing is necessary for the decrease in I_h.

As a test of this hypothesis, 3 Hz pairing was repeated with fast glutamatergic transmission blocked by including CNQX (10 μM) and D, L-APV/(+)-MK-801 (50 μM/10 μM) in the extracellular saline (Fig. 7*A*). Under these conditions, with all ionotropic receptors blocked, presumably only mGluR receptors are activated during the pairing protocol. In the presence of CNQX/APV/MK-801, 3 Hz pairing resulted in a 66 ± 10% increase in input resistance, similar to the increase seen in the absence of CNQX/APV/MK-801 (Fig. 7*B*). The change in input resistance in the presence of LY3431495 was not significantly different from that seen in the absence of 3 Hz pairing. There was a decrease in f_R after 3 Hz pairing, observed as a leftward shift of the impedance amplitude profile in both control saline and in the presence of ionotropic glutamate antagonists (Fig. 7*C*,*D*). This was not present when mGluRs were blocked by LY341495 or without 3 Hz pairing (Fig. 7*C*,*D*). Because CA1 pyramidal neurons do not express group 2 mGluRs (Luján et al., 1997) and group 3 mGluRs are predominantly presynaptic (Ohishi et al., 1995a,b), we hypothesize that the increase in CA1 pyramidal neuron excitability, via a decrease in I_h, requires the activation of group 1 mGluRs.

As a direct test of this hypothesis, we asked whether the selective group 1 mGluR agonist DHPG could reliably reproduce the changes observed with 3 Hz pairing. Bath application of DHPG

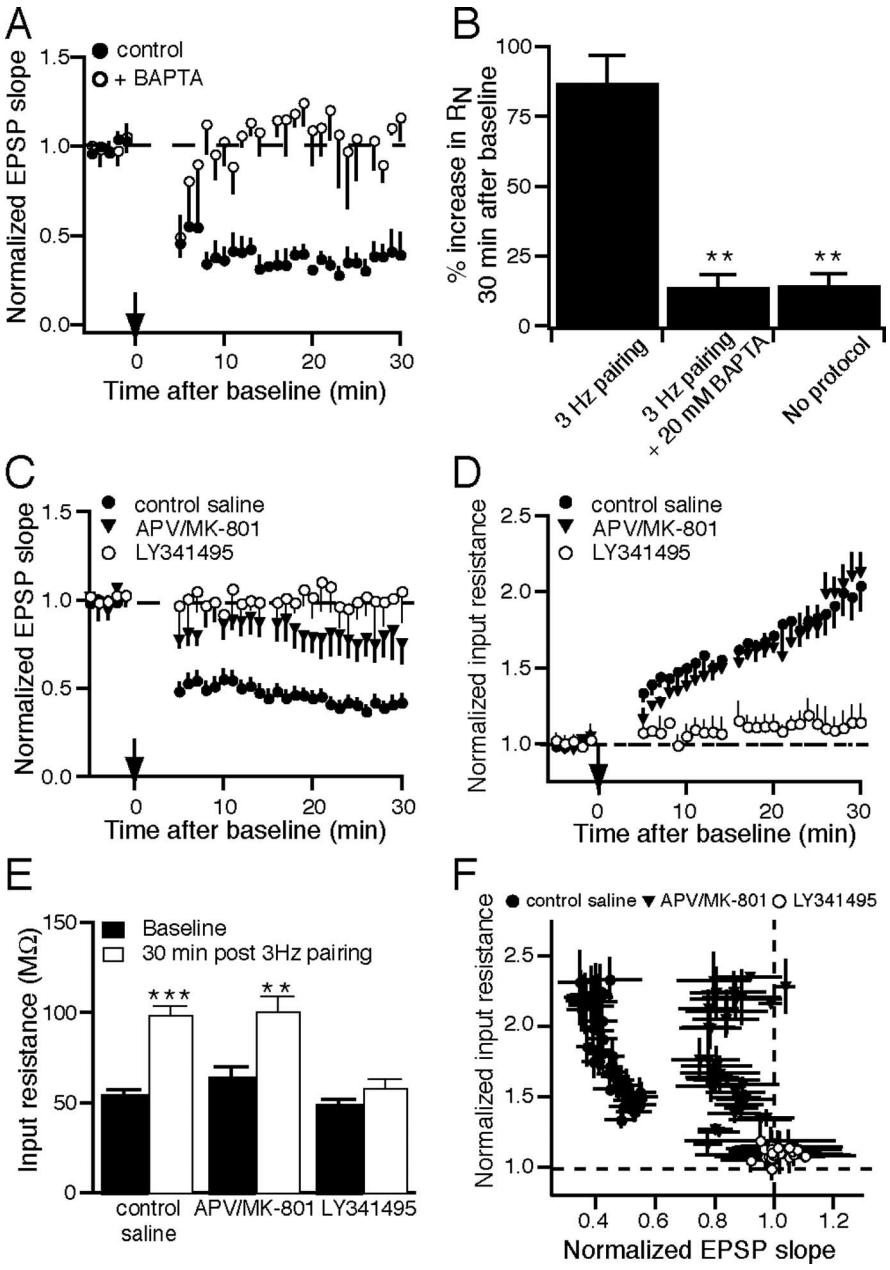

Figure 6. Rises in intracellular calcium and metabotropic glutamate receptor activation are necessary for the increase in excitability after 3 Hz pairing. ***A***, Graph showing the time course and magnitude of the change in EPSP slope after 3 Hz pairing (↓) with control intracellular saline (●) and 20 mM BAPTA in the recording pipette (○; $n = 4$). ***B***, Summary graph showing input resistance measured before and 30 min after 3 Hz pairing with control intracellular saline, 20 mM intracellular BAPTA, and with control intracellular saline but not 3Hz pairing protocol. ***C***, Graph showing the time course and magnitude of the change in EPSP slope after 3 Hz pairing (↓) in control saline (●), with NMDA receptors blocked by 50 μM APV + 10 μM MK-801 (▼); $n = 8$, and with group 1 mGluRs blocked with 100 μM LY341495 ($n = 5$). ***D***, Graph showing the time course and magnitude of the change in input resistance after 3 Hz pairing (↓) in control saline (●), in the presence of APV/MK-801 (▼), and in the presence of LY341495 (○). ***E***, Summary graph showing input resistance measured before and 30 min after 3 Hz pairing in control saline, APV/MK-801, and LY341495. ***F***, Relationship between R_N and EPSP slope after 3 Hz pairing in control saline (●), in the presence of APV/MK-801 (▼), and in the presence of LY341495 (○). Error bars indicate SEM. $^{**}p < 0.01$; $^{***}p < 0.005$ baseline versus 30 min after 3 Hz pairing.

has been used previously in the study of hippocampal mGluR-dependent LTD (Huber et al., 2000). In CA1 pyramidal neurons, application of DHPG is known to increase excitability and is accompanied by depolarization and action potential discharge (Gereau and Conn, 1995). We demonstrated previously that increases in neuronal activity increase I_h via NMDA receptor activation (Fan et al., 2005). We found that 30 min after a 10 min application of DHPG, there was no significant change in R_N. If however, DHPG was applied in the presence of TTX, to block action potentials, or APV, to block NMDA receptors, a significant increase in R_N was observed (Fig. 8*A*). We hypothesized that in control saline, the decrease in I_h by mGluR activation was opposed by AP/NMDA-dependent increases in I_h. To remove this potentially confounding process, DHPG application was performed with NMDA receptors blocked by APV/MK-801. After a 5 min baseline period, DHPG (100 μM) was applied to the slice for 10 min. During DHPG application, CA1 pyramidal neurons depolarized, fired a series of action potentials, and settled at a new resting membrane potential near −40 mV (Fig. 8*B*). After wash out of DHPG, the membrane potential slowly returned to near the baseline value. EPSP slope was significantly decreased 30 min after DHPG washout (baseline, 1.2 ± 0.16 mV/ms; 30 min, 0.8 ± 0.14 mV/ms; $p < 0.005$, $n = 5$) and there was a leftward shift of the impedance amplitude profile (Fig. 8*C*). In agreement with our hypothesis, input resistance was increased (baseline, 54 ± 4 MΩ; DHPG, 106 ± 7 MΩ), sag was decreased (baseline, 19 ± 2%; DHPG, 11 ± 2%; $p < 0.05$), and resonance frequency was decreased (baseline, 3.2 ± 0.5 Hz; DHPG, 1.6 ± 0.3 Hz; $p < 0.05$) 30 min after DHPG application (Fig. 8*D*). The slope of the linear fit of rebound amplitude as a function of membrane potential was also reduced (baseline, −0.2 ± 0.004; 30 min after DHPG, −0.06 ± 0.006; $n = 5$) (Fig. 8*E*). These data further support the hypothesis that activation of group 1 mGluRs increase excitability by decreasing I_h.

Previously, we demonstrated that the decrease in input resistance observed with LTP did not require evoked EPSPs, but in fact, only required b-APs elicited in a theta burst pattern (Fan et al., 2005). Long trains of EPSPs are sufficient to activate mGluRs and induce synaptic plasticity in the hippocampus (Oliet et al., 1997; Huber et al., 2000). We therefore asked whether the downregulation of I_h required the pairing of b-APs and synaptic stimulation. When the stimulation protocol consisted only of b-APs at 3 Hz, there was no significant decrease in EPSP slope. Although synaptic stimulation alone at 3 Hz produced a small depression of EPSP slope, it was significantly less than the LTD caused by 3 Hz pairing (pairing, 62 ± 6%; synaptic only, 24 ± 14%; $p < 0.05$) (Fig. 9*A*). More interestingly, whereas 3 Hz b-APs had no significant effect on input resistance, 3 Hz synaptic stimulation produced an increase in input resistance that was not significantly different from 3 Hz pairing (Fig. 9*B*).

PKC activation is required for downregulation of I_h

Group 1 metabotropic glutamate receptors are coupled to phosphoinositide hydrolysis (Abe et al., 1992; Aramori and Nakanishi, 1992). In the dentate gyrus and area CA1, mGluR-dependent LTD requires the activation of protein kinase C (PKC) (Oliet et al., 1997; Wang et al., 1998). Furthermore, the activation of PKC by neurotensin receptors can inhibit I_h in the substantia nigra (Cathala and Paupardin-Tritsch, 1997). We therefore tested the hypothesis that PKC activation is necessary for the downregulation of I_h. Bath application of the PKC inhibitor GF109203X (10 μM) blocked the 3 Hz pairing induced LTD (control, 38 ± 5% vs 97 ± 12%, $p < 0.001$) (Fig. 9*C*). Block of PKC by GF109203X also prevented the leftward shift of the impedance amplitude profile after 3 Hz pairing (Fig. 9*D*). Block of PKC by GF109203X significantly reduced the increase in input resistance, decrease in voltage sag, and decrease in resonance frequency measured 30 min after 3 Hz pairing (Fig. 9*E*).

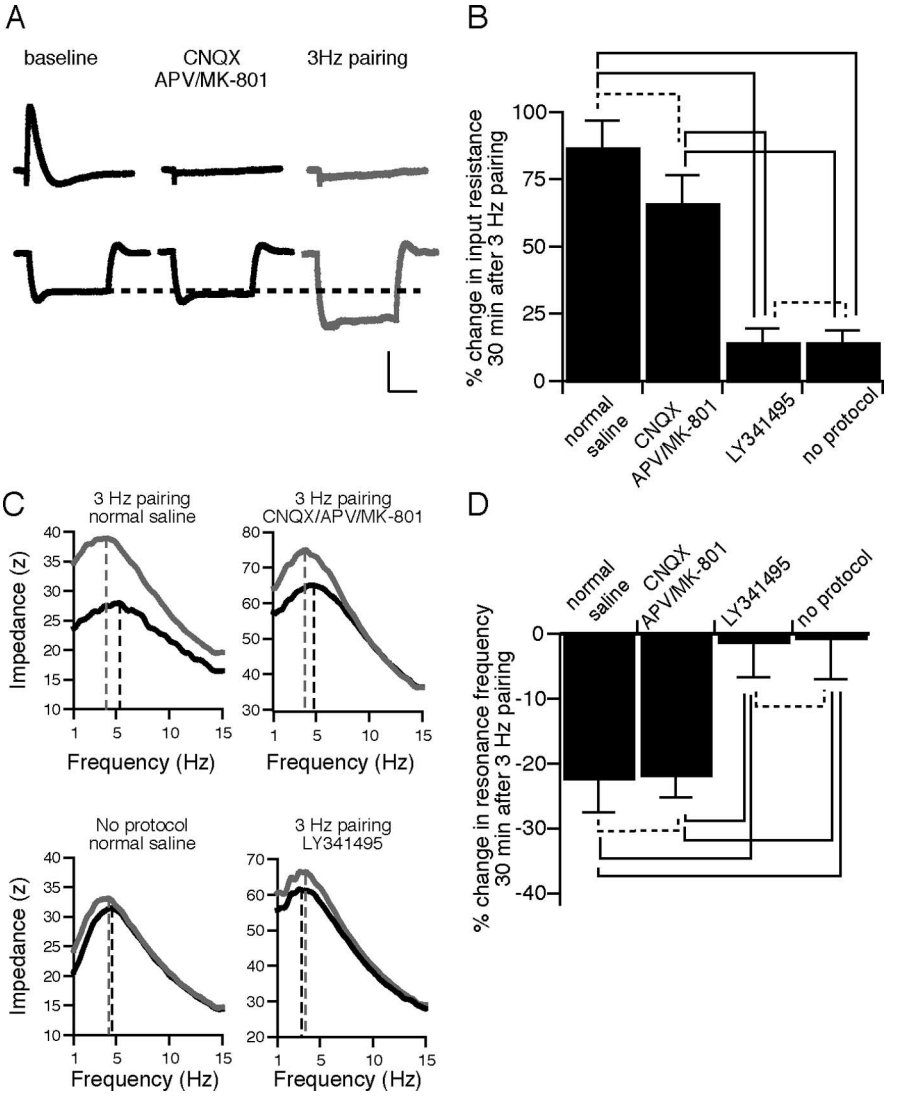

Figure 7. Decreases in I_h persist with ionotropic glutamate receptors blocked during 3 Hz pairing. ***A***, Representative traces of EPSPs (top) and input resistance (bottom, hyperpolarizing voltage deflections in response to −50 pA) in control saline (baseline), with 10 μM CNQX, 50 μM APV, and 10 μM MK-801 present to block ionotropic glutamate receptors, and 30 min after 3 Hz pairing (gray). There was no significant change in R_N after wash in of CNQX/APV/MK-801. Calibration: 4 mV, 75 or 200 ms (for EPSP and R_N traces respectively). ***B***, Summary graph showing the normalized change in R_N 30 min after 3 Hz pairing in the four experimental groups (control saline, $n = 20$; CNQX/APV/MK-801, $n = 4$; LY341495, $n = 5$; no induction protocol, $n = 7$). ***C***, Representative impedance amplitude profiles before (black) and after (gray) 3 Hz pairing from four types of experiments: control (top left), with ionotropic glutamate receptors blocked (top right), without 3 Hz pairing (bottom left), and with metabotropic glutamate receptors blocked (bottom right). The dashed lines indicate the maximum impedance (resonance frequency). ***D***, Summary graph showing the normalized change in resonance frequency 30 min after 3 Hz pairing in the four experimental groups. Error bars indicate SEM. Solid lines, $p < 0.05$; dashed lines, $p > 0.05$.

Discussion

Changes in neuronal output from a given input are thought to form the cellular basis of learning and memory (Bear, 1996). We demonstrated previously that a long-lasting decrease in excitability, accompanying certain forms of LTP, was caused by the activity-dependent upregulation of I_h (Fan et al., 2005). In this study, we show that there is an activity-dependent increase in neuronal excitability that accompanies 3 Hz stimulation-induced LTD. Similar to the decrease in excitability after LTP (Fan et al., 2005), the increase in excitability occurs gradually over the course of several minutes. This increase in excitability is dependent on the activation of group 1 metabotropic glutamate receptors and protein kinase C. Furthermore, changes in electrophysiological characteristics indicative of I_h (e.g., input resistance, voltage sag, temporal summation, and resonance frequency), coupled with sensitivity to the h-channel blocker ZD7288, strongly support the conclusion that a long-lasting downregulation of I_h underlies this increase in excitability.

Early demonstrations of increases in excitability after LTD focused on changes in EPSP–spike (E/S) coupling. Bernard and Wheal (1995) reported an increase in E/S coupling accompanying LTD. Although both the extracellularly recorded EPSP (fEPSP) and population spike (PS) are reduced after LTD, the relationship between fEPSP slope and PS amplitude is increased. Because all of our experiments used intracellular recordings, our observations were localized to a single CA1 neuron and cannot address any changes in the population of neurons. Two potential mechanisms explaining increased E/S coupling are decreased inhibitory drive and/or a change in action potential threshold (Wilson, 1981; Abraham et al., 1987; Taube and Schwartzkroin, 1988; Chavez-Noriega et al., 1989; Hess and Gustafsson, 1990). Because changes in excitability occurred after LTD with inhibition blocked by bicuculline and picrotoxin and we did not observe a significant change in action potential threshold, we suggest that the decrease in I_h during LTD may be a separate phenomenon.

The h-channel blocker ZD7288 has reported presynaptic effects on synaptic transmission. Chevaleyre and Castillo (2002) reported that bath application of ZD7288 (1–50 μM) reduced Schaffer collateral EPSP amplitude and increased paired-pulse facilitation, consistent with a decrease in presynaptic release probability. However, this same report also demonstrated that

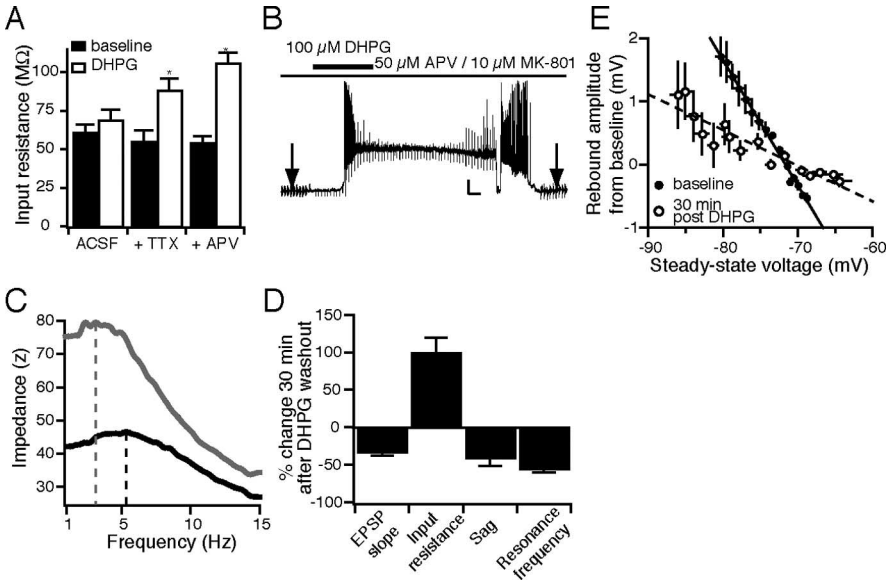

Figure 8. DHPG application mimics the 3 Hz pairing effects on intrinsic excitability. ***A***, Summary data showing that block of action potentials with TTX or NMDA receptors with APV reveals an mGluR-dependent increase in input resistance. ***B***, Representative recording showing the change in CA1 pyramidal neuron excitability that occurs during and after a 10 min application of DHPG (100 μM). Arrows indicate the time of the baseline and post DHPG measurements. The downward deflection near the end of the trace was caused by a brief increase in holding current to monitor series resistance. Calibration: 40 mV, 500 s. ***C***, Representative impedance amplitude profile before (black) and after (gray) a 10 min application of 100 μM DHPG in the presence of APV/MK-801 produced a leftward shift of the resonance frequency (dashed lines). ***D***, Summary data showing the change in input resistance, sag, and resonance frequency 30 min after 10 min DHPG application ($n = 5$). ***E***, Summary graph showing rebound potential amplitude as a function of membrane potential before (●) and after (○) DHPG application. Error bars indicate SEM. *$p < 0.05$ versus baseline.

bath application of 50 μM ZD7288 (more than twice the concentration used in this study) did not significantly reduce EPSC amplitude over a 15 min application although completely blocked postsynaptic I_h. Furthermore, the time required to observe a significant effect of ZD7288 on release probability was longer than most of the recordings in this study (>60 min).

Activity-dependent plasticity has traditionally been associated with increases and decreases in synaptic strength (Bliss and Collingridge, 1993; Bear and Malenka, 1994). Previously, activity-dependent changes in voltage-dependent channels have been shown to alter intrinsic excitability (Turrigiano et al., 1994; Desai et al., 1999; Golowasch et al., 1999; Frick et al., 2004; Fan et al., 2005). There are several reports of changes in intrinsic excitability associated with LTP from cortex, cerebellum, and hippocampus (Aizenman and Linden, 2000; Wang et al., 2003; Cudmore and Turrigiano, 2004; Frick et al., 2004; Fan et al., 2005; Xu et al., 2005). Our results demonstrate the first report of activity-dependent changes in intrinsic excitability accompanying LTD.

Mechanism

Prolonged low-frequency synaptic stimulation or asynchronous pairing of EPSPs and action potentials in the hippocampus leads to both NMDAR and mGluR activation (Oliet et al., 1997; Normann et al., 2000). Our results suggest that although both receptors can contribute to the depression of EPSPs, only mGluR activation is necessary for activity-dependent decreases in I_h.

Previous reports of mGluR activation on CA1 pyramidal neuron excitability examined the changes in intrinsic properties during agonist application (Desai and Conn, 1991; Gereau and Conn, 1995). In contrast, we report persistent effects up to 30 min after either 3 Hz stimulation or DHPG application. Metabotropic glutamate receptor agonists can increase excitability by inhibiting several intrinsic potassium conductances including I_{AHP} and I_{leak} (Charpak et al., 1990; Desai and Conn, 1991; Gereau and Conn, 1995). Although we cannot exclude the possibility that the spike afterhyperpolarization is reduced, changes in I_{AHP} cannot explain our results because I_{AHP} does not contribute to any of the electrophysiological parameters altered after 3 Hz stimulation. Our results are also not explained by a persistent decrease in I_{leak} because the increase in input resistance after 3 Hz pairing was voltage dependent (Fig. 5*B*).

We report a decrease in maximum resonance frequency (f_R) without a significant change in the voltage where that maximum occurs (V_B) (Fig. 4*F*). A hyperpolarizing shift in $V_{1/2}$ would shift the f_R versus V_m curve to the left and increase its peak amplitude, without an overall reduction in f_R values across V_m. A decrease in g_{max} would reduce the peak f_R without shifting V_B (supplemental Fig. 2, available at www.jneurosci.org as supplemental material). Given that there is a decrease in the maximum f_R, not an increase, that the shift in V_B is within sampling limits (5 mV), and that there is an overall reduction in f_R across voltages, we suggest that decreases in the maximum conductance and not shifts in $V_{1/2}$ underlie the activity-dependent downregulation of I_h. However, additional experiments are needed to rigorously test this hypothesis.

Protein kinase C is activated during the induction of mGluR-mediated LTD in the hippocampus and dentate gyrus (Oliet et al., 1997; Wang et al., 1998). We found that block of PKC activation prevented the downregulation of I_h and the subsequent increase in excitability. Activation of group 1 mGluRs is coupled to phosphoinositide hydrolysis and the generation of diacylglycerol and inositide-1,4,5-trisphosphate (IP_3), resulting in the activation of protein kinase C and IP_3-sensitive Ca^{2+} stores respectively (Abe et al., 1992; Aramori and Nakanishi, 1992). Because the increase in excitability by 3 Hz pairing was completely blocked by intracellular BAPTA but not by NMDA antagonists, we suggest that Ca^{2+} release from stores may be involved in the downregulation of I_h.

Impact on neuronal function

We previously showed that an enhancement of I_h counterbalances the increase in synaptic strength during LTP to normalize neuronal firing (Fan et al., 2005). This would prevent saturation of neuronal output caused by potentiation of synaptic transmission (Abraham et al., 2001). For modulation of I_h to be an effective homeostatic mechanism, it is essential that I_h regulate neuronal output in the opposite direction as well. Without a mechanism to maintain action potential firing, uncontrolled LTD could lead to a complete loss of neuronal output. Therefore, a homeostatic mechanism to prevent this hypoexcitability should exist. If increases in I_h serve as the regulator of neuronal firing during potentiated synaptic transmission, then decreases in I_h may serve a similar function during depressed synaptic transmission.

In this study, we demonstrated that 3 Hz pairing-induced LTD was accompanied by increased neuronal firing caused by increased input resistance. A reduction in I_h would thus make naive synapses of the cell more effective at generating action potentials. One possibility is that the overall result of LTD induction is not just to reduce the contribution of the stimulated synapses, but also to increase the signal from the nonstimulated pathways. One consequence of I_h downregulation is an increase in EPSP decay time and increased in temporal summation (Magee, 1998). This would prolong the depolarization produced by an EPSP and increase the likelihood of action potential generation caused by the integration of multiple inputs. We found that the decay time of nondepressed EPSPs was significantly increased by 20% similar to depressed EPSPs (Fig. 3). Under these conditions, depressed inputs would have a reduced role in AP generation whereas nondepressed inputs would have a greater role. From our previously published results on theta-burst pairing (TBP) LTP, the opposite can be hypothesized: TBP-LTP selects for the potentiated synapses. In TBP-LTP a subset of synapses becomes potentiated whereas the entirety of the synaptic inputs become less effective because of a global increase in I_h (Narayanan and Johnston, 2007). Under these conditions, only the potentiated synapses would be more effective at generating action potentials. By modulating dendritic I_h in concert with synaptic strength, a neuron cannot only increase or decrease the likelihood of action potential generation, but also select which sets of inputs contribute to that AP generation.

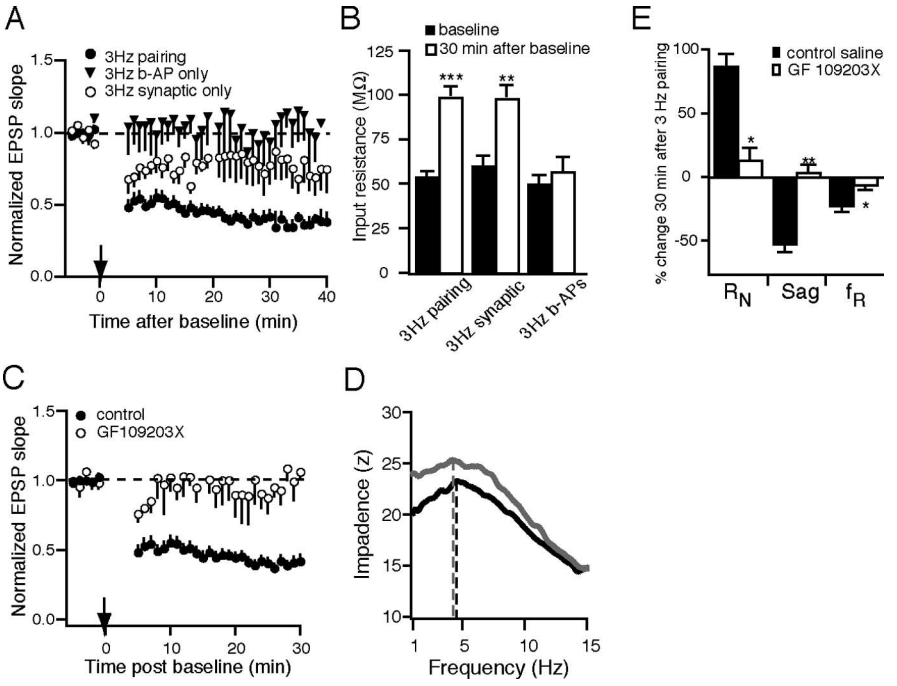

Figure 9. The decrease in I_h requires only synaptic stimulation and the activation of protein kinase C. ***A***, Graph showing the time course and magnitude of the change in EPSP slope after 3 Hz pairing (●), a 3 Hz train of b-APs alone (▼; $n = 5$), and a 3 Hz train of synaptic stimulation alone (○; $n = 7$). ***B***, Summary data showing the change in input resistance (R_N) 30 min after the indicated protocol. All data are expressed as mean ± SEM. $^{**}p < 0.01$; $^{***}p < 0.005$ baseline versus 30 min post 3 Hz protocol. ***C***, Graph showing the time course and magnitude of the change in EPSP slope after 3 Hz pairing in control saline (●) and in the presence of 10 μM GF109203X (○; $n = 5$). ***D***, Representative impedance amplitude profile before (black) and after (gray) 3 Hz pairing in the presence of GF109203X. ***E***, Summary data showing the change in input resistance, sag, and resonance frequency 30 min after 3 Hz pairing in control saline and in the presence of GF109203X. Error bars indicate SEM $^{*}p < 0.05$; $^{**}p < 0.01$ control saline versus GF109203X.

In conclusion, we have shown that activity-dependent bidirectional plasticity is not restricted to synapses. We demonstrated that decreases in synaptic strength are counterbalanced by concomitant increases in intrinsic excitability. We demonstrated previously that increases in synaptic strength were counterbalanced by decreases in intrinsic excitability (Fan et al., 2005). This bidirectional regulation of intrinsic excitability is mediated by the activity-dependent increase or decrease in a single voltage-gated conductance, I_h.

References

Abbott LF, Nelson SB (2000) Synaptic plasticity: taming the beast. Nat Neurosci 3 [Suppl]:1178–1183.

Abe T, Sugihara H, Nawa H, Shigemoto R, Mizuno N, Nakanishi S (1992) Molecular characterization of a novel metabotropic glutamate receptor mGluR5 coupled to inositol phosphate/Ca^{2+} signal transduction. J Biol Chem 267:13361–13368.

Abraham WC, Gustafsson B, Wigström H (1987) Long-term potentiation involves enhanced synaptic excitation relative to synaptic inhibition in guinea-pig hippocampus. J Physiol (Lond) 394:367–380.

Abraham WC, Mason-Parker SE, Bear MF, Webb S, Tate WP (2001) Heterosynaptic metaplasticity in the hippocampus in vivo: a BCM-like modifiable threshold for LTP. Proc Natl Acad Sci USA 98:10924–10929.

Aizenman CD, Linden DJ (2000) Rapid, synaptically driven increases in the intrinsic excitability of cerebellar deep nuclear neurons. Nat Neurosci 3:109–111.

Aponte Y, Lien CC, Reisinger E, Jonas P (2006) Hyperpolarization-activated cation channels in fast-spiking interneurons of rat hippocampus. J Physiol (Lond) 574:229–243.

Aramori I, Nakanishi S (1992) Signal transduction and pharmacological characteristics of a metabotropic glutamate receptor, mGluR1, in transfected CHO cells. Neuron 8:757–765.

Bear MF (1996) A synaptic basis for memory storage in the cerebral cortex. Proc Natl Acad Sci USA 93:13453–13459.

Bear MF, Malenka RC (1994) Synaptic plasticity: LTP and LTD. Curr Opin Neurobiol 4:389–399.

Bliss TVP, Collingridge GL (1993) A synaptic model of memory: long-term potentiation in the hippocampus. Nature 361:31–39.

Bolshakov VY, Siegelbaum SA (1994) Postsynaptic induction and presynaptic expression of hippocampal long-term depression. Science 264:1148–1152.

Brager DH, Capogna M, Thompson SM (2002) Short-term synaptic plasticity, simulation of nerve terminal dynamics, and the effects of protein kinase C activation in rat hippocampus. J Physiol (Lond) 541:545–559.

Cathala L, Paupardin-Tritsch D (1997) Neurotensin inhibition of the hyperpolarization-activated cation current (Ih) in the rat substantia nigra pars compacta implicates the protein kinase C pathway. J Physiol (Lond) 503:87–97.

Charpak S, Gähwiler BH, Do KQ, Köpfel T (1990) Potassium conductances in hippocampal neurons blocked by excitatory amino-acid transmitters. Nature 347:765–767.

Chavez-Noriega LE, Bliss TV, Halliwell JV (1989) The EPSP-spike (E-S) component of long-term potentiation in the rat hippocampal slice is modulated by GABAergic but not cholinergic mechanisms. Neurosci Lett 104:58–64.

Chen X, Johnston D (2004) Properties of single voltage-dependent K+ channels in dendrites of CA1 pyramidal neurones of rat hippocampus. J Physiol (Lond) 559:187–203.

Chevaleyre V, Castillo PE (2002) Assessing the role of Ih channels in synap-

tic transmission and mossy fiber LTP. Proc Natl Acad Sci USA 99:9538–9543.

Christie BR, Magee JC, Johnston D (1996) The role of dendritic action potentials and Ca^{2+} influx in the induction of homosynaptic long-term depression in hippocampal CA1 pyramidal neurons. Learn Mem 3:160–169.

Cudmore RH, Turrigiano GG (2004) Long-term potentiation of intrinsic excitability in LV visual cortical neurons. J Neurophysiol 92:341–348.

Desai MA, Conn PJ (1991) Excitatory effects of ACPD receptor activation in the hippocampus are mediated by direct effects on pyramidal cells and blockade of synaptic inhibition. J Neurophysiol 66:40–52.

Desai NS, Rutherford LC, Turrigiano GG (1999) Plasticity in the intrinsic excitability of cortical pyramidal neurons. Nat Neurosci 2:515–520.

DiFransesco D (1993) Pacemaker mechanisms in cardiac tissue. Annu Rev Physiol 55:455–472.

Dudek SM, Bear MF (1992) Homosynaptic long-term depression in area CA1 of hippocampus and effects of *N*-methyl-D-aspartate receptor blockade. Proc Natl Acad Sci USA 89:4363–4367.

Fan Y, Fricker D, Brager DH, Chen X, Lu HC, Chitwood RA, Johnston D (2005) Activity-dependent decrease of excitability in rat hippocampal neurons through increases in I(h). Nat Neurosci 8:1542–1551.

Frick A, Johnston D (2005) Plasticity of dendritic excitability. J Neurobiol 64:100–115.

Frick A, Magee J, Johnston D (2004) LTP is accompanied by an enhanced local excitability of pyramidal neuron dendrites. Nat Neurosci 7:126–135.

Gasparini S, DiFrancesco D (1997) Action of the hyperpolarization-activated current (I_h) blocker ZD 7288 in hippocampal CA1 neurons. Pflügers Arch 435:99–106.

Gereau RW, Conn PJ (1995) Roles of specific metabotropic glutamate receptor subtypes in regulation of hippocampal CA1 pyramidal cell excitability. J Neurophysiol 74:122–129.

Golowasch J, Abbott LF, Marder E (1999) Activity-dependent regulation of potassium currents in an identified neuron of the stomatogastric ganglion of the crab Cancer borealis. J Neurosci 19:RC33.

Hess G, Gustafsson B (1990) Changes in field excitatory postsynaptic potential shape induced by tetanization in the CA1 region of the guinea-pig hippocampal slice. Neuroscience 37:61–69.

Huber KM, Kayser MS, Bear MF (2000) Role for rapid dendritic protein synthesis in hippocampal mGluR-dependent long-term depression. Science 288:1254–1257.

Huber KM, Gallagher SM, Warren ST, Bear MF (2002) Altered synaptic plasticity in a mouse model of fragile X mental retardation. Proc Natl Acad Sci USA 99:7746–7750.

Hutcheon B, Yarom Y (2000) Resonance, oscillation and the intrinsic frequency preferences of neurons. Trends Neurosci 23:216–222.

Hutcheon B, Miura RM, Puil E (1996) Subthreshold membrane resonance in neocortical neurons. J Neurophysiol 76:683–697.

Kaczorowski CC, Disterhoft J, Spruston N (2007) Stability and plasticity of intrinsic membrane properties in hippocampal CA1 pyramidal neurons: effects of internal anions. J Physiol (Lond) 578:799–818.

Kim J, Jung SC, Clemens AM, Petralia RS, Hoffman DA (2007) Regulation of dendritic excitability by activity-dependent trafficking of the A-type K+ channel subunit Kv4.2 in hippocampal neurons. Neuron 54:933–947.

Kole MH, Hallermann S, Stuart GJ (2006) Single Ih channels in pyramidal neuron dendrites: properties, distribution, and impact on action potential output. J Neurosci 26:1677–1687.

Luján R, Roberts JD, Shigemoto R, Ohishi H, Somogyi P (1997) Differential plasma membrane distribution of metabotropic glutamate receptors mGluR1 alpha, mGluR2 and mGluR5, relative to neurotransmitter release sites. J Chem Neuroanat 13:219–241.

Lüthi A, Bal T, McCormick DA (1998) Periodicity of thalamic spindle waves is abolished by ZD7288, a blocker of Ih. J Neurophysiol 79:3284–3289.

Maccaferri G, McBain CJ (1996) The hyperpolarization-activated current (Ih) and its contribution to pacemaker activity in rat CA1 hippocampal stratum oriens-alveus interneurones. J Physiol (Lond) 497:119–130.

Magee JC (1998) Dendritic hyperpolarization-activated currents modify the integrative properties of hippocampal CA1 pyramidal neurons. J Neurosci 18:7613–7624.

Magee JC (1999) Dendritic lh normalizes temporal summation in hippocampal CA1 neurons. Nat Neurosci 2:508–514.

Magee JC, Johnston D (1995) Characterization of single voltage-gated Na+ and Ca^{2+} channels in apical dendrites of rat CA1 pyramidal neurons. J Physiol (Lond) 487:67–90.

Magee JC, Johnston D (1997) A synaptically controlled, associative signal for Hebbian plasticity in hippocampal neurons. Science 275:209–213.

Malenka RC, Bear MF (2004) LTP and LTD: an embarrassment of riches. Neuron 44:5–21.

Matsuda H, Saigusa A, Irisawa H (1987) Ohmic conductance through the inwardly rectifying K channel and blocking by internal Mg^{2+}. Nature 325:156–159.

Mulkey RM, Malenka RC (1992) Mechanisms underlying induction of homosynaptic long-term depression in area CA1 of the hippocampus. Neuron 9 (5):967–975.

Narayanan R, Johnston D (2007) Long-term potentiation in rat hippocampal neurons is accompanied by spatially widespread changes in intrinsic oscillatory dynamics and excitability. Neuron, in press.

Normann C, Peckys D, Schulze CH, Walden J, Jonas P, Bischofberger J (2000) Associative long-term depression in the hippocampus is dependent on postsynaptic *N*-type Ca^{2+} channels. J Neurosci 20:8290–8297.

Ohishi H, Akazawa C, Shigemoto R, Nakanishi S, Mizuno N (1995a) Distribution of the mRNAs for L-2-amino-4-phosphobutyrate-sensitive metabotropic glutamate receptors, mGluR4 and mGluR7, in the rat brain. J Comp Neurol 360:555–570.

Ohishi H, Nomura S, Ding YQ, Shigemoto R, Wada E, Kinoshita A, Li JL, Neki A, Nakanishi S, Mizuno N (1995b) Presynaptic localization of a metabotropic glutamate receptor, mGluR7, in the primary afferent neurons: an immunohistochemical study in the rat. Neurosci Lett 202:85–88.

Oliet SHR, Malenka RC, Nicoll RA (1997) Two distinct forms of long-term depression coexist in CA1 hippocampal pyramidal cells. Neuron 18:969–982.

Pape HC (1996) Queer current and pacemaker: the hyperpolarization-activated cation current in neurons. Annu Rev Physiol 58:299–327.

Poolos NP, Migliore M, Johnston D (2002) Pharmacological upregulation of h-channels reduces the excitability of pyramidal neuron dendrites. Nat Neurosci 5:767–774.

Rammes G, Palmer M, Eder M, Dodt HU, Zieglgänsberger W, Collingridge GL (2003) Activation of mGlu receptors induces LTD without affecting postsynaptic sensitivity of CA1 neurons in rat hippocampal slices. J Physiol (Lond) 546:455–460.

Selig DK, Lee HK, Bear MF, Malenka RC (1995) Reexamination of the effects of MCPG on hippocampal LTP, LTD, and depotentiation. J Neurophysiol 74:1075–1082.

Taube JS, Schwartzkroin PA (1988) Mechanisms of long-term potentiation: EPSP/spike dissociation, intradendritic recordings, and glutamate sensitivity. J Neurosci 8:1632–1644.

Turrigiano G, Abbott LF, Marder E (1994) Activity-dependent changes in the intrinsic properties of cultured neurons. Science 264:974–977.

Turrigiano GG, Nelson SB (2000) Hebb and homeostasis in neuronal plasticity. Curr Opin Neurobiol 10:358–364.

Wang Y, Wu J, Rowan MJ, Anwyl R (1998) Role of protein kinase C in the induction of homosynaptic long-term depression by brief low frequency stimulation in the dentate gyrus of the rat hippocampus in vitro. J Physiol (Lond) 513:467–475.

Wang Z, Xu NL, Wu CP, Duan S, Poo MM (2003) Bidirectional changes in spatial dendritic integration accompanying long-term synaptic modifications. Neuron 37:463–472.

Wilson RC (1981) Changes in translation of synaptic excitation to dentate granule cell discharge accompanying long-term potentiation. I. Differences between normal and reinnervated dentate gyrus. J Neurophysiol 46:324–338.

Xu J, Kang N, Jiang L, Nedergaard M, Kang J (2005) Activity-dependent long-term potentiation of intrinsic excitability in hippocampal CA1 pyramidal neurons. J Neurosci 25:1750–1760.